# An Experimental Study of Ability of Similarity Theory to Predict Water Evaporation Rate for Different Convection Regimes

**Amin Jodat**

Bojnourd Branch, Islamic Azad University, Bojnourd, Iran

Email: amin.jodat@Yahoo.com, Tel: 0098-0584-2237546

***Abstract*– In the present study, the applicability of standard model (similarity theory) has been experimentally investigated for natural, forced and combined convection regimes. A series of experimental measurements are carried out over a wide range of water temperatures and air velocities for $0.01 \leq Gr_m/Re^2 \leq 100$ in a heated rectangular pool. The results show that for forced convection regime due to ripples appear on the water free surface, similarity theory under predicts the evaporation rate. In the free convection regime, the similarity theory considers correctly the effects of both vapor pressure difference and vapor density difference. For mixed convection regime, although the similarity theory is not able to predict the mild non-linearity behavior between water evaporation rate and vapor pressure difference, but satisfactory results can be achieved by using the modified correlation proposed in this study.**

***Keywords*–** Evaporation Rate, Forced Convection, Mixed Convection, Free Convection and Similarity Theory

## I. INTRODUCTION

Evaporation of water into air streams is important from heat and mass transfer points of view. Based on the flow regimes, the water evaporation may be divided into different categories. The convection mechanisms (natural or forced convection) and the flow regimes (laminar or turbulent flow) influence the rate of evaporation [1], [2]. In attention to numerous applications of water evaporation in many aspects of nature and industrial engineering, considerable efforts have been made to correlate water evaporation rate from free water surface into the both still and moving air [1], [3] - [5]. The most commonly used correlations are: 1) the correlations based on the John Dalton's theory [6] and 2) the correlations based on the analogy between heat and mass transfer [7].

Dalton stated that water evaporation is proportional to the difference in vapor pressure at the surface of the water and in the ambient air and that; the velocity of the wind affects this proportionality. Numerous researchers have expressed their results based on Dalton's description [3, 8-10].

The research is financed by Bojnourd Branch, Islamic Azad University, No. 09-11-1/18786, Iran

Also, the nonlinear dependency of evaporation rate ($\dot{m}_e$) on the vapor pressure difference has been considered by many researchers [1], [5], [11] - [15] and has become the basis of considerable modifications on Dalton's theory. The modified Dalton based correlation accounting for this nonlinearity is as follows:

$$\dot{m}_e = (C_1 + C_2 V)\left(P_{v,s} - \varphi P_{v,\infty}\right)^n / h_{fg} \qquad (1)$$

where $\dot{m}_e$ is the water evaporation rate, $P_{v,s}$ and $P_{v,\infty}$ are the saturated vapor pressure at the free surface and at the ambient, respectively. $\varphi$ is the relative humidity and $h_{fg}$ is the latent heat of evaporation. $C_1$, $C_2$ and n are the constants which are determined from multiple parameters embedded in these values, like the area of water bodies, their shapes and different convection regimes [16]. Table 1 shows a summary of the proposed correlations which are mentioned in literature.

The other approach to predict the evaporation rate is the well-known similarity theory which is a standard basis for predicting evaporation rate from a free water surface [7], [17]. Similarity theory states that convective heat and mass transfer are completely analogous phenomena under certain conditions [17]. They are analogous when the two following conditions apply [7]:

- The mass flow from the surface must be diffusion. In general, this requires that the concentration of the diffusing species be low.
- The diffusional mass flux must be low enough that it does not affect the imposed velocity field.

However, applying this analogy for high surface temperatures and concentrations [7] or capillary porous media containing a liquid [18], [19] is not valid. Also the failure of the similarity theory for natural convection in a vertical channel of finite length when flow reversal occurs has been pointed out by Lee and Parikh [20]. However, Based on this theory, the convective heat transfer correlations in the form of the Nusselt number can be employed to evaluate the mass transfer rate if the Prandtl number is replaced by the Schmidt number and the Grashof number replaced by the mass transfer Grashof number [17], [21], [22].

Despite the extensive studies on development of the similarity theory, the necessity of a comparison between this approach with experimental data in different flow regimes is evident. The present study of evaporation measurements has been motivated by the need to assess the applicability of similarity theory results at a wide range of convection regimes ($0.01 \leq Gr_m/Re^2 \leq 100$). The measurements are performed in a heated water pool inside a wind tunnel. The air velocities used in this investigation ranged from $0.05 m/s$ to $5 m/s$ and the water temperatures considered were from $20°C$ to $55°C$ in approximately $2.5°C$ increments.

## II. MATHEMATICAL CALCULATIONS

Dimensional analysis on the evaporation process reveals that the mass transfer conservation equation is analogous to the heat conservation equation [1]. Therefore, if the corresponding boundary conditions are similar, then the solution of these equations will also be similar. The dimensionless governing equations are as follows [17]:

$$\rho^* \frac{DT^*}{Dt} = \frac{1}{Re\,Pr} \nabla^*.(k^* \nabla^* T^*) \tag{2}$$

$$\rho^* \frac{DC^*}{Dt} = \frac{1}{Re\,Sc} \nabla^*.(D^* \nabla^* C^*) \tag{3}$$

where $\rho^*$, $k^*$, $D^*$, $T^*$ and $C^*$ are the dimensionless density, conductivity, mass diffusivity, temperature and concentration fields, respectively. Pr and Sc are the Prandtl and Schmidt numbers defined as [17]:

$$Pr = \frac{\nu}{\alpha}, Sc = \frac{\nu}{D_{H2o,air}} \tag{4}$$

where $\nu$, $\alpha$ and $D_{H2o,air}$ are the kinematic viscosity, thermal and mass diffusivities, respectively. The dimensionless parameters mentioned in equations (2) and (3) play a significant role in the evaporation of water. The Nusselt and Sherwood numbers which are widely used to evaluate the heat and mass transfer rates can be defined as a function of Reynolds, Prandtl and Schmidt numbers [7]:

$$Nu = \frac{hL}{k} = f(Re, Pr) \tag{5}$$

$$Sh = \frac{g_{m,H2o} L}{\rho D_{H2o,air}} = g(Re, Sc) \tag{6}$$

where $L$ is the characteristic length of the evaporation surface, $h$ and $g_{m,H2o}$ are the heat convection coefficient and the mass transfer coefficient, respectively. In addition, the binary diffusion coefficient can be estimated as follows [7]:

$$D_{H2o,air} = 1.87 \times 10^{-10} \left[\frac{T^{2.072}}{P}\right] \tag{7}$$

In order to calculate the mass transfer coefficient, the analogy between heat and mass transfer results in the following expression [7]:

$$g_{m,H2o} = \frac{\dot{m}_e}{m_{f\,H2O,s} - m_{f\,H2O,\infty}} \tag{8}$$

where $m_{f\,H2O,\infty}$ and $m_{f\,H2O,s}$ are the mass fractions of water within the air and in the saturated form, respectively:

$$m_{f\,H2O,\infty} = \frac{18.02\, X_{H2O,\infty}}{[18.02\, X_{H2O,\infty} + 28.96(1 - X_{H2O,\infty})]} \tag{9}$$

$$m_{f\,H2O,s} = \frac{18.02\, X_{H2O,s}}{[18.02\, X_{H2O,s} + 28.96(1 - X_{H2O,s})]} \tag{10}$$

in which $X_{H2O}$ is the vapor mole fraction as a function of the vapor pressure ($P_{H2O}$) and the atmosphere pressure ($P_{atm}$) as:

$$X_{H2O} = \frac{P_{H2O}}{P_{atm}} \tag{11}$$

In order to evaluate the saturated vapor pressure ($P_{v,s}$) as a function of temperature, the following relation may be used [21]:

$$P_{v,s} = 10^5 \exp\left[65.832 - 8.2 \ln(T_s) + 5.717 \times 10^{-3} T_s - \frac{7235.46}{T_s}\right] \tag{12}$$

where $T_s$ is the free surface temperature.

The evaporation rate can be calculated from the Sherwood number using [7]:

$$\dot{m}_e = Sh \frac{\rho D_{H2o,air}}{L} (m_{f\,H2O,s} - m_{f\,H2O,\infty}) \tag{13}$$

The Sherwood number must be defined for each convection regime. In order to determine which convection regime is more dominant, the following expression may be used:

$$\frac{Gr_m}{Re^2} = \frac{\text{Natural Convection Strength}}{\text{Forced Convection Strength}} \tag{14}$$

where $Gr_m$ and Re are the Grashof and Reynolds numbers, respectively, which can be expressed as:

$$Gr_m = \frac{\bar{\rho}_g (\rho_{g,s} - \rho_{g,\infty}) g L^3}{\mu^2} \tag{15}$$

$$Re = \frac{\bar{\rho}_g V L}{\mu} \tag{16}$$

where $\rho_{g,s}$ and $\rho_{g,\infty}$ are the densities of moist air at the surface of water and at the ambient, respectively. V, is the wind velocity, $\mu$ is the air viscosity and L is the characteristic length of the test chamber. The density of the moist air at the free surface is estimated as the sum of the partial densities of vapor ($\rho_{v,s}$) and dry air ($\rho_{a,s}$) as [22]:

$$\rho_{g,s} = \rho_{v,s} + \rho_{a,s} \tag{17}$$

In addition, the mean mixture of air in the boundary layer ($\bar{\rho}_g$) define as [22]:

$$\bar{\rho}_g = \frac{\rho_{g,s} + \rho_{g,\infty}}{2} \tag{18}$$

In order to calculate the density of moist air, the perfect gas equation is used.

For the forced convection flow regimes, $\mathrm{Gr_m}/\mathrm{Re}^2$ is much less than one while for the free convection, $\mathrm{Gr_m}/\mathrm{Re}^2$ is much greater than one. In addition, if $\mathrm{Gr_m}/\mathrm{Re}^2$ is almost one, the flow regime is a combination of both natural and forced convection regimes [7].

In the mass transfer analogy the Sherwood number for the free and forced convection turbulent flow regimes is defined as [7]:

$$\mathrm{Sh_{free}} = 0.14(\mathrm{Gr_m}.\mathrm{Sc})^{\frac{1}{3}} \tag{19}$$

$$\mathrm{Sh_{forced}} = 0.03\ \mathrm{Sc}^{\frac{1}{3}}\ \mathrm{Re}^{0.8} \tag{20}$$

It should be noted that the flow regime was turbulent in the free convection regime since the mass based Grashoff number (equation (15)) ranged from $2.1 \times 10^8$ to $6.7 \times 10^9$. Also, due to the existence of a series of baffles which were placed in the upstream end of the wind tunnel, the air flow regime in the forced convection regime was turbulent. Therefore, equations (19) and (20) are valid for the turbulent flow regime.

For the mixed convection flow regime ($\mathrm{Gr_m}/\mathrm{Re}^2 \cong 1$) the Sherwood number is given by the following nonlinear combination [7]:

$$\mathrm{Sh_{mixed}} = \mathrm{Sh_{free}}\left[1 + \left(\frac{\mathrm{Sh_{forced}}}{\mathrm{Sh_{free}}}\right)^a\right]^{\frac{1}{a}} \tag{21}$$

where $a$ is an exponent which can vary in the range of one and two [1].

## III. EXPERIMENTAL SETUP AND MEASUREMENTS

The experimental measurements were carried out in a test chamber with internal dimensions of 150×100×100 cm. The pond depth of the test chamber was 25 cm. A schematic of the test chamber is shown in figure 1. The large size of the evaporation pan of this investigation allowed reducing convective edge effects. Small pans have a greater portion of their interior surface affected by convection due to density gradients around the pan edges [3]. In order to reduce the heat loss via conduction, the pond was made up of MDF-board[1] and the whole test chamber was isolated using the polystyrene panels of 5 cm in thickness. An aluminum foil tape was used within the interior surfaces to reduce the radiative heat loss and prevent water vapor absorption.

Two immersion heaters were installed near the bottom of the pan to elevate the water temperature to the desired conditions. They were low heat flux heaters with 2500 watts of total power each. The heaters were made of nichrome wire encased in PTFE[2] spaghetti tubing.

A draw-thru centrifugal fan was used to exhaust the air and control the wind velocity within the chamber. The draw-thru fans have the advantage of reducing the turbulent effects on the evaporation rate. The evaporation rate was evaluated based on two methods. First, the flow rate and the difference between the inlet and outlet absolute humidity were used. Second, with the help of a small pan which was connected to the main pond via a siphon tube [8]. The evaporation rate was calculated based on weighing this small pan using a digital scale in a 10-minute period of time. The maximum capacity and the resolution of the scale was about 4 kg and 0.01 g, respectively; However, when the evaporation rate was too slow the measurements were recorded in hourly basis time interval.

The mean surface water temperature was measured by averaging the temperatures of eight T-type thermocouples that were placed 4 cm below the water surface. The pan was divided into eight equal square sections and one thermocouple was placed in the centre of each section. The water temperatures considered in this investigation ranged from 20°C to 55°C in approximately 2.5°C increments. A thermoregulation system was used to guarantee a temperature oscillation of water of about ±0.1°C from the fixed value.

Air relative humidity was measured by two sensors placed at the inlet and outlet of the wind tunnel, 25 cm above the water surface. In addition, the air temperature was measured by a thermocouple located over the mid-point of the evaporation pan.

The air velocity within the chamber was measured using thermal anemometer, at nine locations across the water surface at about 15 mm from water surface, and the maximum deviation observed was less than 10 %. The average air velocities considered were 0.05, 0.1, 0.3, 0.9, 1.5, 2, 4 and 5m/s. The inlet air temperature and relative humidity were controlled using a conventional air conditioning system. The specifications of the devices are presented in Table 2. All measurements were recorded using a PC data acquisition system. However, all the measuring instruments had been calibrated before the experiments were performed.

## IV. RESULTS AND DISCUSSIONS

A wide range of flow regimes namely free, mixed and

[1]Medium- Density Fiberboard
[2]Protec Fluoropolymer Heaters

forced convection ($0.01 \leq \mathrm{Gr_m}/\mathrm{Re}^2 \leq 100$) is studied to reveal the abilities of similarity theory. This range of $\mathrm{Gr_m}/Re^2$ is produced using air average velocities of $0.05$, $0.1$, $0.3$, $0.9$, $2$, $4$ and $5\,\mathrm{m/s}$ and the water temperatures from $20°\mathrm{C}$ to $55°\mathrm{C}$. Having produced this range of $\mathrm{Gr_m}/Re^2$, we have then compared our experimental results with the similarity theory results. Figure 2 shows the effect of vapor pressure difference and air stream velocity on the free water surface evaporation rate. The results presented in this figure cover all free, mixed and forced convection regimes investigated in this study. It can be seen that an increase in the vapor pressure difference/air velocity increases the evaporation rate. The data of this figure have been used to evaluate the capability of similarity theory in separate convection regimes:

### *A. Forced Convection Regime*

Fig. 3 demonstrates the influence of the vapor pressure difference and wind velocity on the evaporation rate for the forced convection regime ($0.01 \leq \mathrm{Gr_m}/\mathrm{Re}^2 \leq 0.15$). The experimental results show that the evaporation rate increases nonlinearly with the increase of vapor pressure difference. This occurs because at high evaporation rates (forced convection regime) the vapor density boundary layer is thicker than that expected due to the existence of the surface vapor emission. As the vapor pressure difference increases the surface emission is more intense which slows down the increasing rate of evaporation. This is in accord with the experimental data of Marek and Straub [12], Tang and Etzion [5] and Al-Shamimiri [14].

Fig. 4 compares the evaporation rate measurements with the results of similarity theory. It can be seen that the similarity theory not only is not able to predict the nonlinear dependency between water evaporation rate and vapor pressure difference but under predicts the evaporation rate due to the assumptions exist in this theory that some of them are not perfectly true [7]. One of the main assumptions is that the water evaporation surface must be completely smooth, while at high air velocities, ripples appear on the free surface of the water. These ripples act like surface roughness and thus augment the turbulent transport of water vapor [3].

### *B. Mixed Convection Regime*

The effect of the vapor pressure difference on the evaporation rate for the mixed convection regime ($0.15 \leq \mathrm{Gr_m}/\mathrm{Re}^2 \leq 25$) has been shown in figure 5. As seen in the figure, the slope of the curves, which are fitted to the experimental data, increases with the vapor pressure difference; which is in accordance with Paukan [1], Moghiman [13] and Boetler [11]. Also the comparison between the experimental data and the similarity theory results [7] are depicted in figure 6, for the air velocity of $\mathrm{V} = 0.9\ \mathrm{m/s}$ with the corresponding range of ($0.3 \leq \mathrm{Gr_m}/\mathrm{Re}^2 \leq 3$). Based on the experimental data of this figure and the evaporation correlations in the literature [1], it appears that the exponent *a* in equation (21) should have a value between 1 and 2 but no specific value have ever presented for this exponent in the literature. Attention is now paid to find the parameters that the exponent *a* depends on. Our experimental data show that the exponent *a* can be represented more accurately if it is considered to be a function of dimensionless product: $\mathrm{Gr_m}/\mathrm{Re}^2$. The functional form which is best fits to our experimental results is found to have the following form: (22)

$$\frac{Sh_{mixed}}{Sh_{free}} = \left(1 + \left(\frac{Sh_{forced}}{Sh_{free}}\right)^{-0.042\left(\frac{Gr_m}{\mathrm{Re}^2}\right)^2 + 0.583\frac{Gr_m}{\mathrm{Re}^2} + 1.182}\right)^{1\Big/\left(-0.042\left(\frac{Gr_m}{\mathrm{Re}^2}\right)^2 + 0.583\frac{Gr_m}{\mathrm{Re}^2} + 1.182\right)}$$

The comparison of the experimental data with the presented correlation (equation (22)) is shown in Fig. 7. This figure shows the ratio of $\mathrm{Sh_{total}}/\mathrm{Sh_{free}}$ calculated based on the experimental evaporation data versus the ratio of $\mathrm{Sh_{force}}/\mathrm{Sh_{free}}$. The free and forced convection components of Sherwood number are calculated from equations (19) and (20), respectively. The good agreement between the experimental data and the proposed model which can be observed in this figure, shows that this modification can make the exponent *a* more accurately in the mixed convection regime.

### *C. Free Convection Regime*

Fig. 8, shows the comparison between the measured evaporation data with the results of the similarity theory [7] as a function of vapor pressure difference. The air velocity is less than $0.1\ \mathrm{m/s}$ and $\mathrm{Gr_m}/\mathrm{Re}^2 > 25$. It can be seen that the results of experimental data and similarity theory are close but do not follow a specific trend. The scattering of the results show that the evaporation rate is not a simple function of vapor pressure difference in the free convection regime. In fact, in the free convection regime both the vapor pressure difference and the density difference between the water surface and the ambient air affect the evaporation rate. This dependency of the evaporation rate on the density difference has also been reported in the literature [8], [23].

To take into account the effects of both vapor pressure difference and density difference, in Figure 9, $\dot{\mathrm{m}}_\mathrm{e}/\Delta\mathrm{P}$ for similarity theory and experimental data are plotted as a function of the density difference. The small discrepancy between the experimental data and the similarity theory is due to the fact that at low density differences the sideways movements of air and stray air currents which are not considered in the similarity theory affect the evaporation rate. These effects have also been observed by Shah [23], Sharpley [24] and Boelter [11]. Their measurements of repeated tests were scattered at low density differences about ±15%.

In Fig. 10, the ratio of total Sherwood number to the Sherwood number for the free convection regime $\mathrm{Sh_{total}}/\mathrm{Sh_{free}}$ versus $\mathrm{Gr_m}/\mathrm{Re}^2$ has been shown. In this figure, the total Sherwood number and the free convection Sherwood number for all data collected in the experiments were calculated using equation (6) and equation (19) respectively.

Then the variations of the ratio of $\mathrm{Sh_{total}}/\mathrm{Sh_{free}}$ are plotted versus $\mathrm{Gr_m}/\mathrm{Re}^2$ and the best fit to this curve found to have the following form:

$$\frac{Sh_{total}}{Sh_{free}} = 1.441 - 0.345 \ln\left(\frac{\mathrm{Gr_m}}{Re^2}\right) + 0.22\left[\ln\left(\frac{\mathrm{Gr_m}}{Re^2}\right)\right]^2 - 0.037\left[\ln\left(\frac{\mathrm{Gr_m}}{Re^2}\right)\right]^3 \quad (23)$$

Equation (23) is valid for a wide range of convection regimes ( $0.01 \le \mathrm{Gr_m}/\mathrm{Re}^2 \le 100$ ). This dimensionless correlation allows the results of this study to be extended to other evaporating conditions (variation in surface geometry and airflow conditions) rather than those described here.

## V. CONCLUSIONS

In the present paper, the validity of the similarity theory results to water evaporation rate calculations, are assessed by performing experimental measurements in different evaporation regimes. A wide range of $\mathrm{Gr_m}/\mathrm{Re}^2$ ($0.01 \le \mathrm{Gr_m}/\mathrm{Re}^2 \le 100$) is achieved by applying different air velocities and water temperatures on a heated water pool in a wind tunnel. Based on the presented results, the following conclusions may be drawn:

- For forced convection regime, the escalation rate of evaporation decreased with vapor pressure difference while in the turbulent mixed convection increased.
- For the free convection flow regime, the evaporation rate is a function of not only the vapor pressure difference but also the density difference of the moist air.
- In the free convection regime, the similarity theory considers correctly the effects of both vapor pressure difference and vapor density difference.
- The ability of the similarity theory to predict the water evaporation rate in mixed convection regime can be significantly enhanced if we consider the exponent $a$ in equation (22) as a function of $\mathrm{Gr_m}/Re^2$.
- For forced and mixed convection regimes, the similarity theory is not able to predict the non-linearity between water evaporation rate and vapor pressure difference.
- In present study, a dimensionless correlation using the experimental data of all convection regimes is proposed to cover different water surface geometries and airflow conditions.

## REFERENCES

[1] Paukan, M. T. (1999). An experimental investigation of combined turbulent free and forced evaporation. Experimental Thermal and Fluid Science. 18, 334–340.

[2] Debbissi, C., Orfi, J., and Nasrallah, S. B. (2003). Evaporation of water by free or mixed convection into humid air and superheated steam. International Journal Heat Mass Transfer. 46, 4703–4715. doi:10.1016/ S0017-9310(03)00092-9.

[3] Sartori, E. A. (2000). Critical review on equations employed for the calculation of the evaporation rate from free water surfaces. Solar Energy. 68, 77–89.

[4] Asdrubali, F. A. (2008). Scale model to evaluate water evaporation from indoor swimming pools. Energy Building. 41, 311-319. doi:10.1016/j.enbuild.2008.10.001.

[5] Tang, R. and Etzion, Y. (2004). Comparative studies on the water evaporation rate from a free water surface and that from a free surface. Building Environment. 39, 77–86.

[6] Dalton, J. (1802). Experimental essays on the constitution mixed gases; on the force of steam or vapor from water and other liquids in different temperatures, on evaporation and on the expansion of gases by heat. Mem. Manchester Literature, Physics Science. 535–602(11), 535–602.

[7] Lienhard, J. H. and Lienhard, V. J. H. (2005). A heat transfer textbook, third edition, (Phlogiston Press, New York).

[8] Pauken, M.T., Tang, T.D., Jeter, S.M. and Abdel-Khalik, S.I. (1993). A novel method for measuring water evaporation into still air. ASHRAE Transactions. 99(1), 297–300.

[9] Moghiman, M. and Jodat, A. (2007). Effect of air velocity on water evaporation rate in indoor swimming pools.The Iranian Society of Mechanical Engineers. 8, 19–30.

[10] Rowher, C. (1931). Evaporation from free water surface, US Department of Agriculture in cooperation with Colorado Agricultural Experiment Station, Technical Bulletin. 271, 96-101.

[11] Boetler, L. M. K., Gordon, H. S. and Griffin, J. R. (1946). Free evaporation into air of water from a free horizontal quiet surface. Industrial and Engineering Chemistry. 38(6), 596–600.

[12] Marek, R., Straub, J. (2001). Analysis of the evaporation coefficient and the condensation coefficient of water. International Journal Heat Mass Transfer. 44, 39–53.

[13] Moghiman, M., Jodat, A. (2007). Experimental investigation of water evaporation in indoor swimming pools. International Journal Heat Mass Technology. 25(2), 43–47.

[14] Shamimiri, M. (2002). Evaporation rate as a function of water salinity. Desalination. 150, 189–203.

[15] Hinchley, J. Himus, G. W. (1924). Evaporation in currents of air. Journal Society Chemistry Industrial. 7, 57–63.

[16] Jodat, A. Moghiman, M. (2011). An experimental assessment of the evaporation correlations for natural, forced and combined convection regimes. Journal of Mechanical Engineering Science. 145-153. doi:10.1177/0954406211413961.

[17] Incropera, F. P. and Dewitt, D. P. (2002). Fundamentals of heat and mass transfer. (John Wiley and Sons, New York).

[18] Sergeyev, G.T. (1961). Investigation of external heat and mass transfer with liquid evaporation from a capillary porous body. Inzh. Fiz. Zh. 5,33-37.

[19] Smolsky, B.M. (1962). Heat and mass transfer with liquid evaporation. International Journal of Heat and Mass Transfer. 5, 1011-1021.

[20] Lee, T. Acrivos, A. (1982). Natural convection in a vertical channel with opposing buoyancy forces. International Journal of Heat and Mass Transfer. 25, 499-511.

[21] Boukadida, N. and Nasrallah, S. B. (2001). Mass and heat transfer during water evaporation in laminar flow inside a rectangular channel—validity of heat and mass transfer analogy. International Journal of Thermal Sciences. 40, 67–81.

[22] Iskra, C. R. and Simonson, C. J. (2007) Convective mass transfer coefficient for a hydro dynamically developed airflow in a short rectangular duct. International Journal of Heat and Mass Transfer. 50(11–12), 2376–2393.
[23] Shah, M. M. (2002). Rate of evaporation from undisturbed water pools to quiet air: evaluation of available correlations. International Journal HVAC&R. 8, 125–131.
[24] Boetler, L. M. K., Gordon, H. S. and Griffin, J. R. (1946). Free evaporation into air of water from a free horizontal quiet surface. Industrial and Engineering Chemistry. 38(6), 596–600
[25] Carrier, W. H. (1918).The temperature of evaporation. ASHRAE Transactions. 24, 25–50.

## Nomenclature

| | | | |
|---|---|---|---|
| $D_{H2o,air}$ | binary mass diffusion coefficient$\left(\frac{\mathrm{m}^2}{\mathrm{s}}\right)$ | $T_s$ | free surface temperature (K) |
| $D_h$ | hydraulic diameter of rectangular duct (m) | $t$ | time (h) |
| g | gravitational acceleration $\left(\frac{\mathrm{m}}{\mathrm{S}^2}\right)$ | V | velocity of air $\left(\frac{\mathrm{Kg}}{\mathrm{m}^3}\right)$ |
| $g_{m,H2o}$ | mass transfer coefficient | $W$ | width of the test chamber |
| $\mathrm{Gr_m}$ | mass transfer Grashof number | $X_{H2O}$ | vapor mole fraction |
| $H$ | height of rectangular duct (m) | **Greek symbols** | |
| $h_{fg}$ | enthalpy of vaporization (J/kg) | $\rho$ | density $\left(\frac{\mathrm{Kg}}{\mathrm{m}^3}\right)$ |
| $K$ | thermal conductivity $\left(\frac{\mathrm{W}}{\mathrm{m.K}}\right)$ | $\mu$ | dynamic viscosity $\left(\frac{\mathrm{Ns}}{\mathrm{m}^2}\right)$ |
| $L$ | length of water pan (m) | $\bar{\rho}$ | mean mixture density of air $\left(\frac{\mathrm{Kg}}{\mathrm{m}^3}\right)$ |
| $\dot{m}_e$ | evaporation rate of water $\left(\frac{\mathrm{Kg}}{\mathrm{m}^2.\mathrm{hr}}\right)$ | $\varphi$ | relative humidity |
| $m_{f\ H2O}$ | the mass fractions of water | **Subscripts** | |
| $Nu$ | Nusselt number | g | moist air property including dry air and water vapor |
| $P$ | pressure (Pa) | s | properties at the surface of the water |
| $Pr$ | Prandtl number | free | free convection flow regime |
| $P_{v,s}$ | saturated vapor pressure at the water surface | forced | forced convection flow regime |
| $P_{v,\infty}$ | saturated vapor pressure at the ambient air | mixed | mixed convection flow regime |
| $R^2$ | Correlation coefficient | $\infty$ | average properties at the ambient air |
| $Re$ | Reynolds number | total | sum of free and forced convection component |
| $Sc$ | Schmidt number | | |
| $Sh$ | Sherwood number | | |
| T | temperature (K) | | |

Table 1: Summary of correlations reported in the literature on water evaporation

| Reference | Case | n | Proposed correlation |
|---|---|---|---|
| Dalton (1834) [6] | Still air | 1 | $\dot{m}_e = C(P_{v,s} - \varphi P_{v,\infty})$ |
| Carrier (1918) [25] | Still & moving air | 1 | $\dot{m}_e = 3370(95 + 83.7V)\frac{(P_{v,s} - \varphi P_{v,\infty})}{h_{fg}}$ |
| Rohwer (1931) [10] | Moving air | 1 | $\dot{m}_e = (0.125 + 0.0755V)\left(\frac{P_{v,s} - \varphi P_{v,\infty}}{1000}\right)$ |
| Boelter (1946) [11] | Moving air | 1.22 | $\dot{m}_e = 0.074\left(\frac{P_{v,s} - \varphi P_{v,\infty}}{1000}\right)^{1.22}$ |
| Pauken (1993) [8] | Still air | ----- | $\dot{m}_e = 0.035(C_S - C_a)^{1.237}$ |
| Al-Shamiri (2002) [14] | Moving air | 0.654 | $\dot{m}_e = (0.120836V^{1.478})\left(\frac{P_{v,s} - \varphi P_{v,\infty}}{1000}\right)^{0.654}$ |
| Shah (2002) [23] | Still air | ----- | $\dot{m}_e = C\,\rho_w(\rho_r - \rho_w)^{1/3}\,(W_r - W_w)$ |
| Tang (2004) [5] | Moving air | 0.82 | $\dot{m}_e = 3600(0.2253 + 0.24644V)\frac{(P_{v,s} - \varphi P_{v,\infty})^{0.82}}{h_{fg}}$ |
| Jodat (2011) [16] | Still & moving air | $0.009V^2 - 0.132V + 1.186$ | $\dot{m}_e = a\,(P_{v,s} - \varphi P_{v,\infty})^b$<br>$a = 0.03262V^3 + 0.01814V^2 + 0.04818V + 0.02264$<br>$b = 0.009V^2 - 0.132V + 1.186$ |

Table 2: Specifications of the experimental apparatus

| **Experimental Apparatus** | **Manufacturer** | **Type** | **Range** | **Accuracy** |
|---|---|---|---|---|
| Digital balance | Bel Engineering | Ultra Mark 4000 | 0 to 4 kg | ± 0.01 g |
| Humidity sensors | Ohmic instruments | HS Series | 1% to 99% | ± 1 % RH |
| Temperature sensors | Testo | T-type thermocouples | −50 ℃ to +199.9 ℃ | 0.1 ℃ |
| Thermal anemometer | Testo | Testo 400 | 0 to +20 m/s | ± 0.01 m/s (0 to +1.99 m/s)<br>± 0.02 m/s (+2 to +4.9 m/s)<br>± 0.04 m/s (+5 to +20 m/s) |
| Air conditioning system | Atlas Pars Air Conditioning Co. | AAHC-04 | --- | --- |
| Centrifugal fan | Pars Fan Hoonam | PCB SWS | Maximum capacity-15000 cfm | ---- |

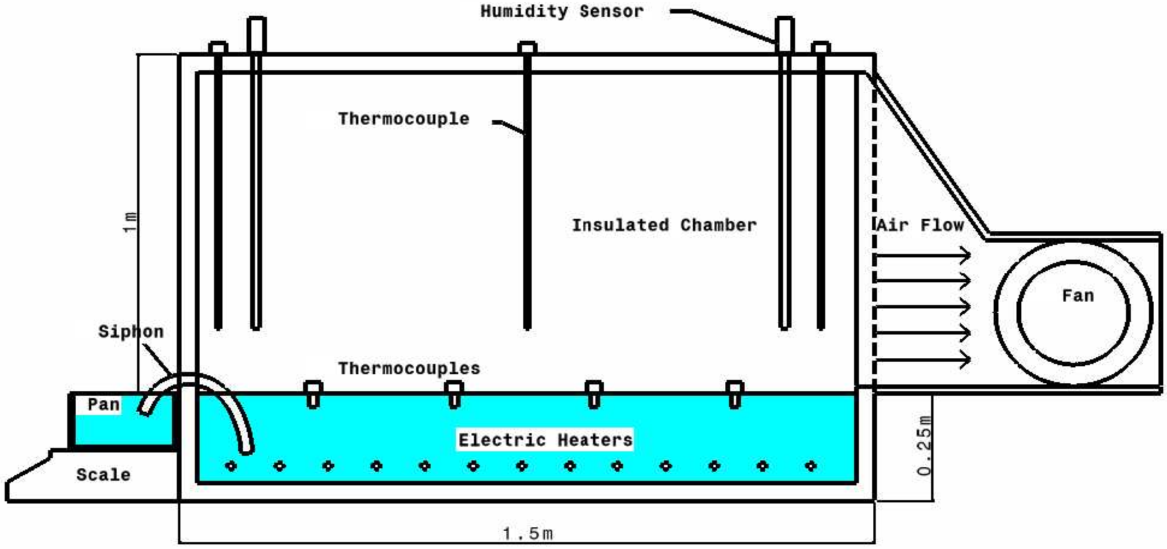


Fig. 1: Experimental test chamber

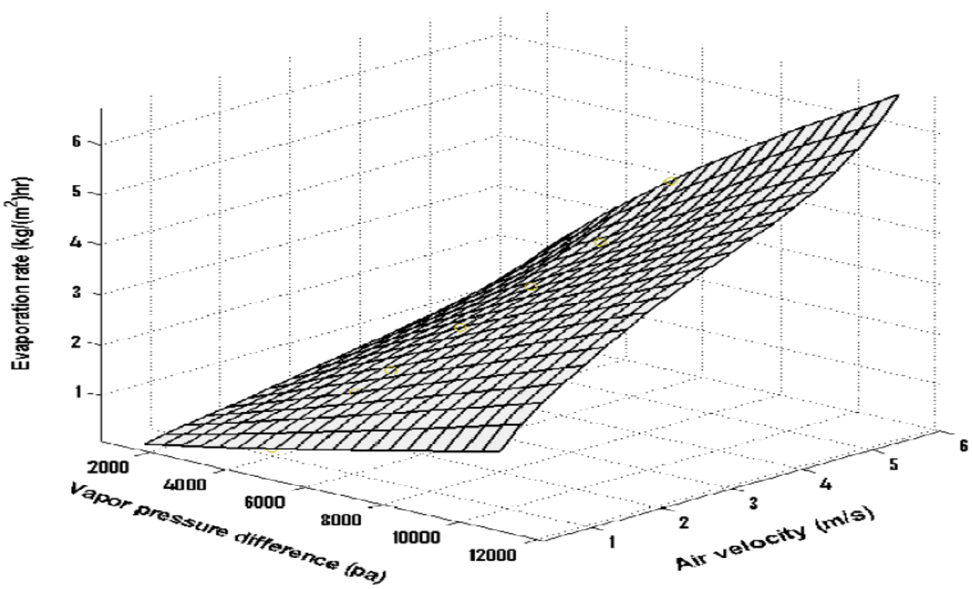


Fig. 2: Effect of vapor pressure difference and air velocity on water surface evaporation rate

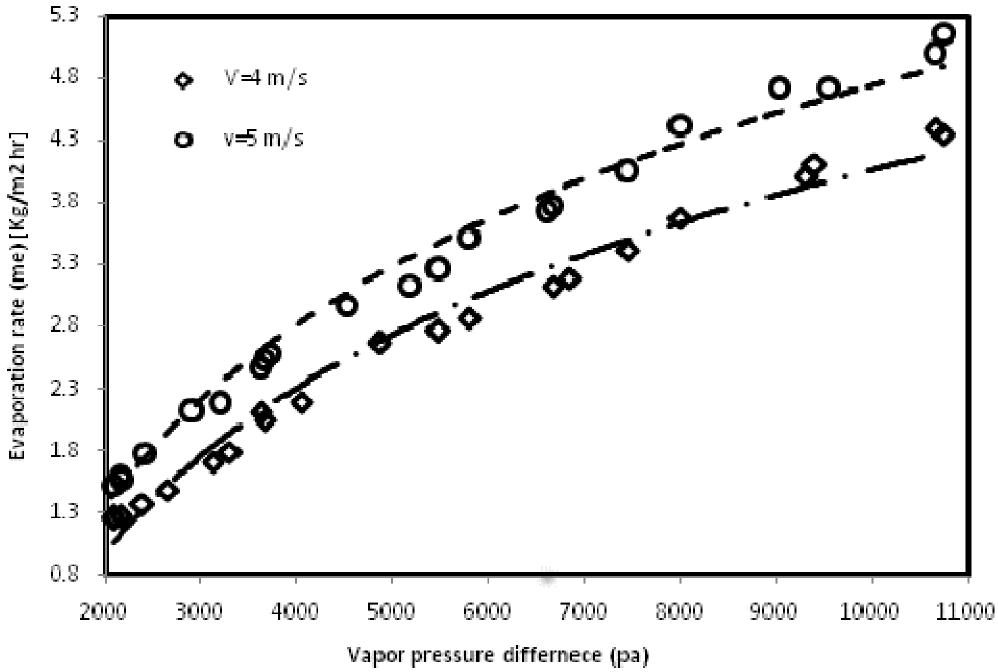


Fig. 3: Evaporation rate versus the vapor pressure difference for various wind velocity of the forced convection regime ($0.01 \leq Gr/Re^2 \leq 0.15$)

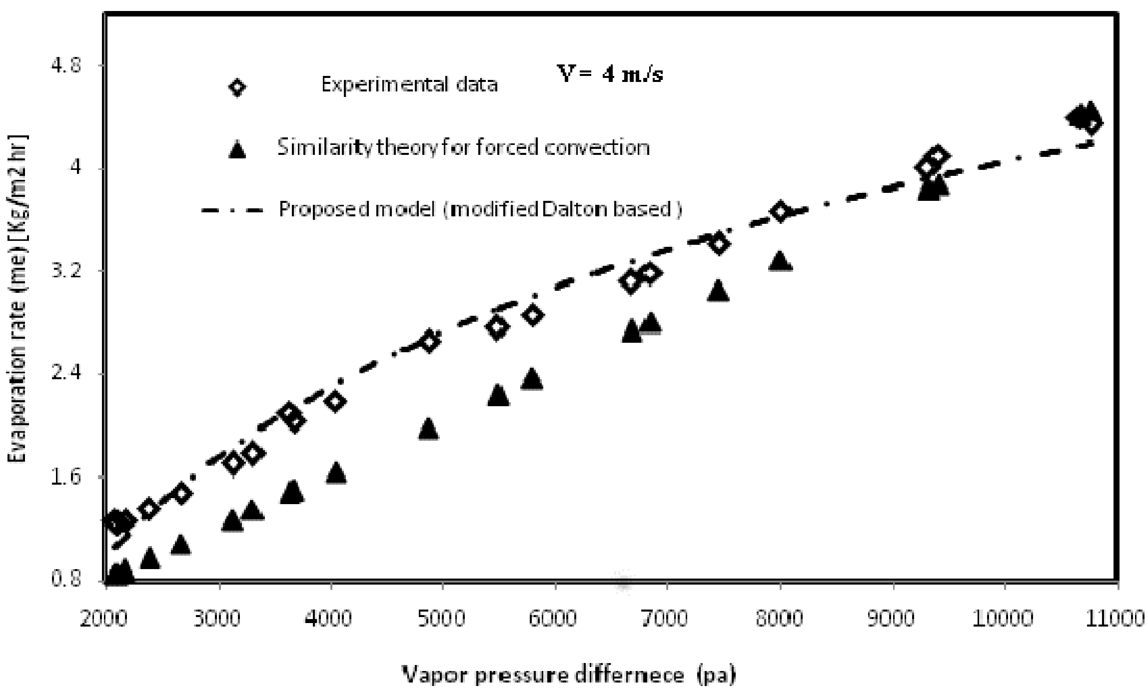


Fig. 4: The comparison between experimental data and similarity theory results for the forced convection regime ($V = \frac{4m}{s}$ and $0.01 \leq Gr_m/Re^2 \leq 0.15$)

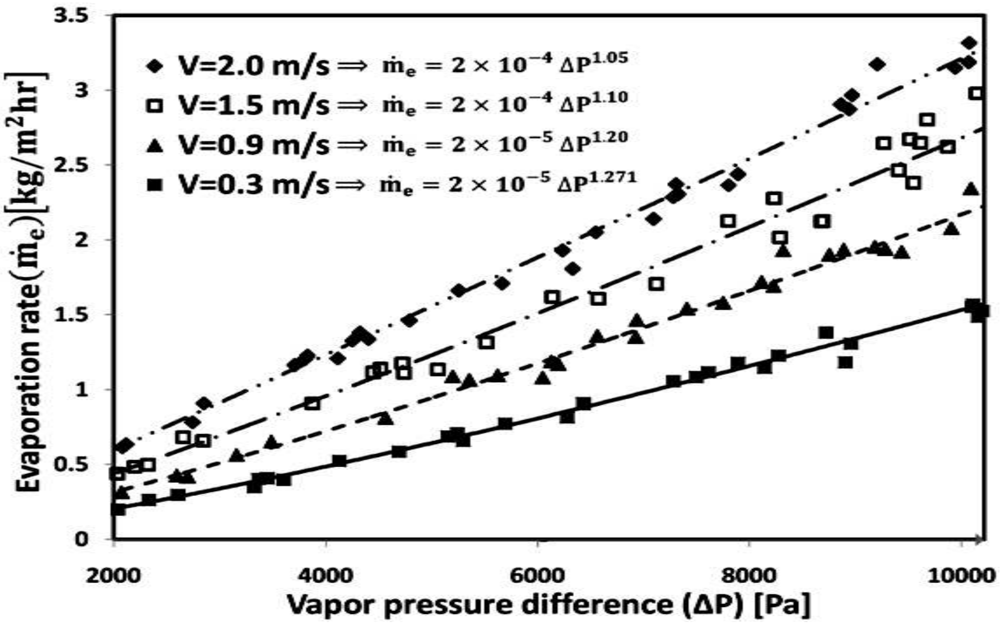


Fig. 5: Evaporation rate against the vapor pressure difference for various wind velocities of the mixed convection regime ($0.15 \leq \mathrm{Gr_m}/\mathrm{Re}^2 \leq 25$)

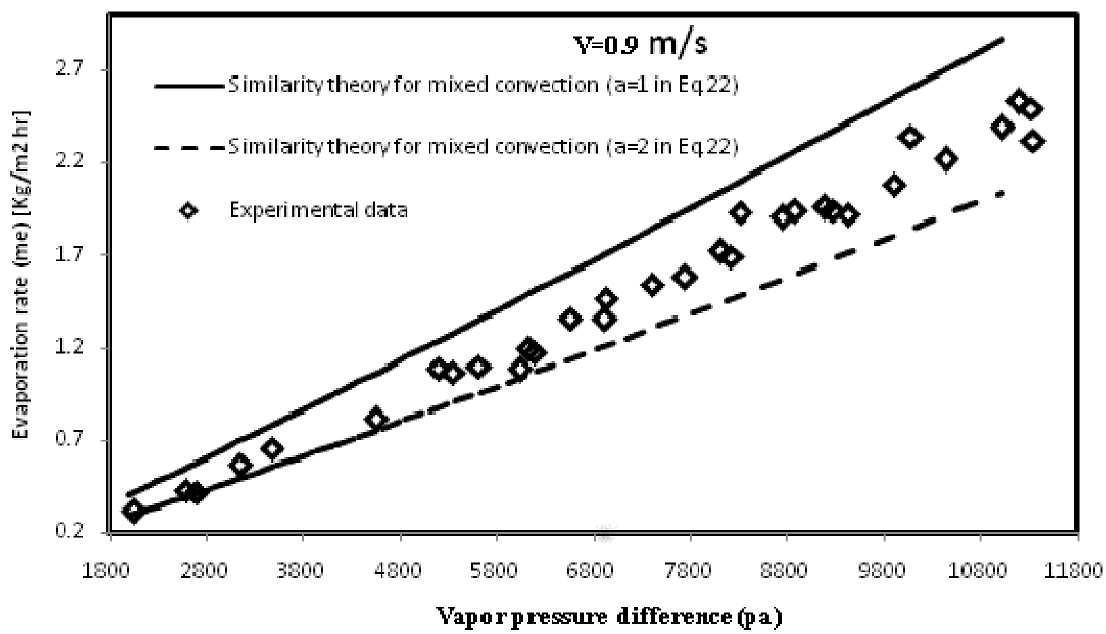


Fig. 6: The comparison between experimental data and similarity theory results for the mixed convection regime ($\mathrm{V} = 0.9\frac{\mathrm{m}}{\mathrm{s}}$ and $0.3 \leq \mathrm{Gr_m}/\mathrm{Re}^2 \leq 3$)

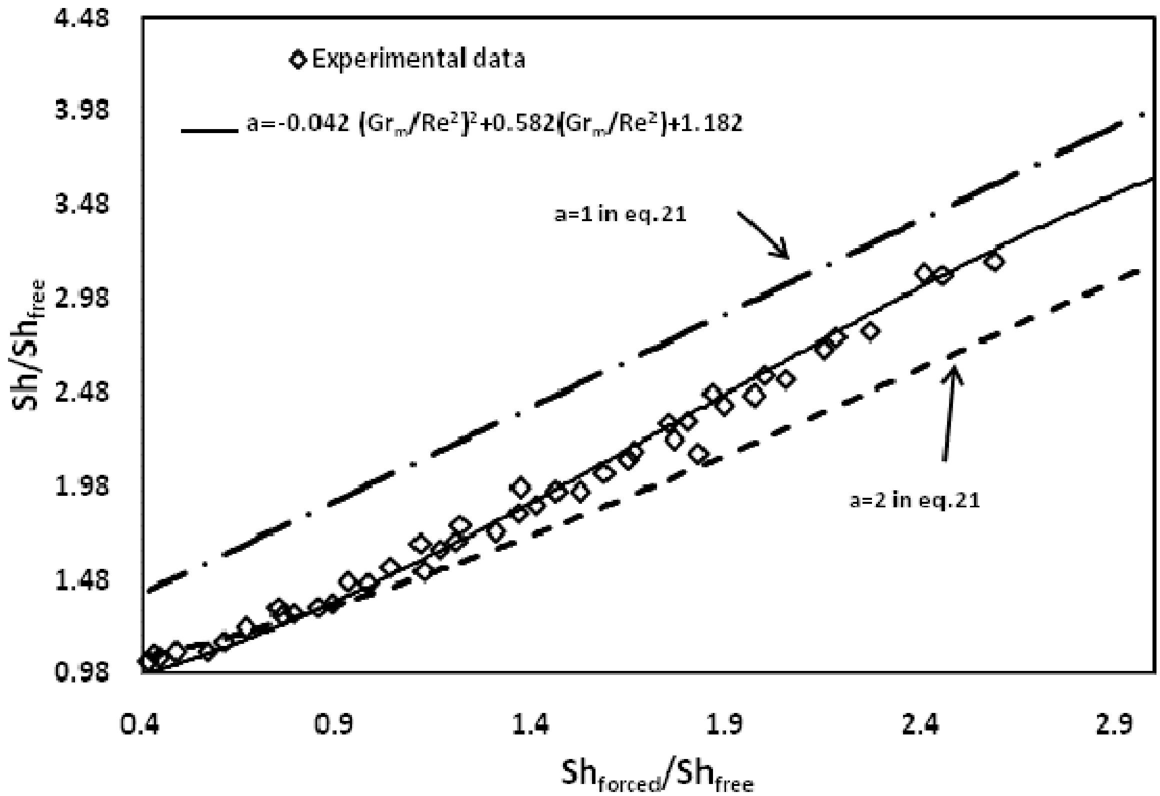


Fig. 7: Dependence of total evaporation rate on the ratio of forced to free convection (Comparison between the experimental data and the similarity theory results)

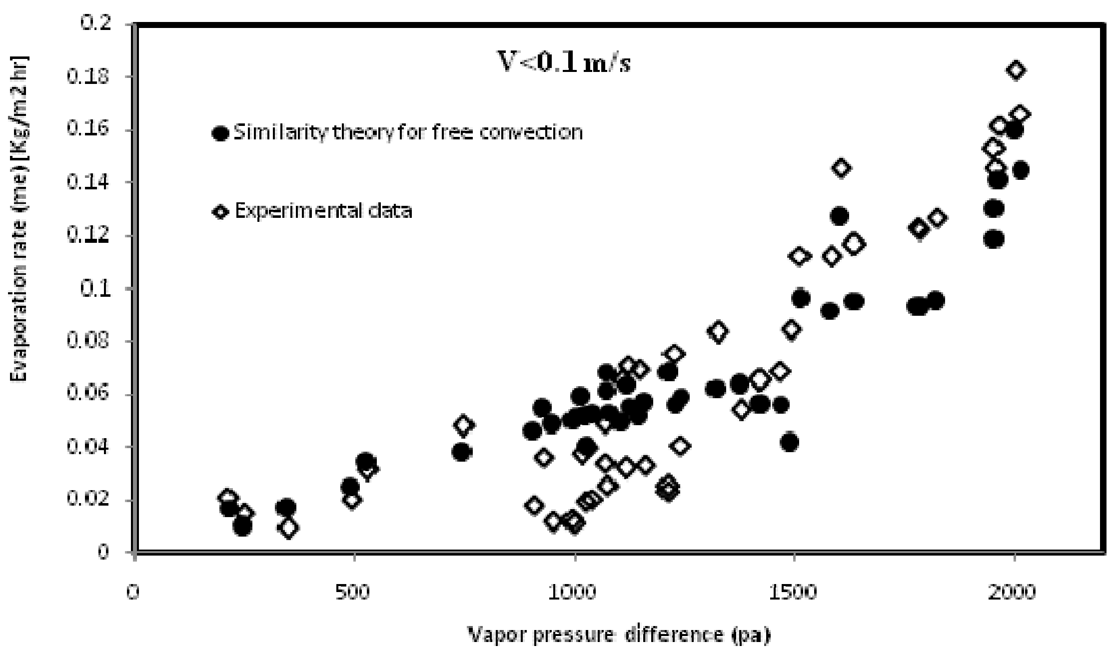


Fig. 8: The comparison between the experimental data, similarity theory results for the free convection regime ($V \leq 0.1$ m/s and $Gr_m/Re^2 \geq 25$)